




PAPER

Deep UV light sensitive $\text{Zn}_{1-x-y}\text{Mg}_x\text{Al}_y\text{O}$ films with fast photoelectric response for SAW photodetectors

To cite this article: M E Kutepov *et al* 2019 *Smart Mater. Struct.* **28** 065024

View the [article online](#) for updates and enhancements.

Deep UV light sensitive $Zn_{1-x-y}Mg_xAl_yO$ films with fast photoelectric response for SAW photodetectors

M E Kutepov¹, V E Kaydashev^{1,2} , G Y Karapetyan¹, T A Minasyan¹,
A V Chernyshev¹, K G Abdulvakhidov¹ , S I Shevtsova¹, E V Glazunova¹,
V A Irkha^{3,4}  and E M Kaidashev¹

¹ Southern Federal University, 200/1 Stachki Ave., 344090 Rostov-on-Don, Russia

² Moscow Institute of Physics and Technology, 9 Institutskiy per., 141701, Dolgoprudny, Russia

³ Don State Technical University, 1 Gagarina St., 344002 Rostov-on-Don, Russia

⁴ Southern Scientific Center RAS, Rostov-on-Don, 344006, Russia

E-mail: kaydashev@gmail.com

Received 30 December 2018, revised 2 April 2019

Accepted for publication 16 April 2019

Published 10 May 2019



CrossMark

Abstract

Optical, structural and photo-electric properties of $Zn_{1-x-y}Mg_xAl_yO$ films on piezoelectric $LiNbO_3$ substrates prepared by PLD method at varied temperatures are studied. The ZnO band gap is enlarged to ~ 5 eV by Mg atoms dosing. The reduced growth temperature of $400^\circ C$ results in lower conductivity of the film. The films grown at $400^\circ C$ – $500^\circ C$ show deep UV photoelectrical response of 0.1–0.2 ms which is 50–100 times faster compared to devices based on films produced at $600^\circ C$ with higher crystallinity. By moderate Al doping and varying the temperature of Zn(Mg, Al)O film growth one may tune the initial sheet conductivity, i.e. the ‘working point’ of UV SAW detector, to the abrupt slopes of $\Gamma(\sigma)$ characteristics, thus, optimizing the sensor sensitivity and response time. The UV ‘light on/off’ sheet conductivity change $\Delta\sigma/\sigma_{dark}$, defining the sensitivity of UV SAW photodetector is tuned between $\sim 22\%$ and $\sim 0.4\%$.

Supplementary material for this article is available [online](#)

Keywords: UV photodetector, pulsed laser deposition (PLD), surface acoustic wave (SAW), zinc oxide (ZnO), ZnMgO, ZnMgAlO

(Some figures may appear in colour only in the online journal)

1. Introduction

ZnO being resistant to proton bombardment and gamma radiation provides new possibilities for UV and deep UV photodetection needed for cosmic applications and ionizing radiation monitoring for which the possibilities of Si based detectors are limited. The band gap of pure ZnO is ~ 3.37 eV and therefore the UV sensitivity of ZnO based photodetectors is limited by the range of ~ 320 – 380 nm. The need to shift the ZnO photoresponse towards deep UV range stimulates the search of new ZnO based materials and the development of new approaches for photodetection.

On the other hand the rapid development of telecommunications requires remotely controlled and autonomous sensors such as passive SAW based transponders, which urges the integration of UV photodetectors to acoustic channel [1–6]. The electric field of the surface acoustic wave propagating along the piezoelectric substrate penetrates to photosensitive semiconductor layer where electron–hole pairs are generated upon light absorption. Acousto-electronic interaction results in (i) the increase of insertion loss for propagating wave and (ii) a reduction of surface wave velocity, which is observed as a phase shift and a SAW arrival delay.

Table 1. Zn(Mg, Al)O films band gap energies, initial sheet conductivity σ_{sh} , fast (τ_{fast}) and slow (τ_{slow}) components of electric photoelectric response kinetics upon the excitation by 15 ns laser pulse at 248 nm and corresponding sheet conductivity change.

Temperature of film growth	Band gap [eV]	Initial sheet conductivity σ_{sh} [Ω^{-1}]	τ_{fast} [μ s]	τ_{slow} [ms]	$\frac{\sigma_{UV ON} - \sigma_{UV OFF}}{\sigma_{UV OFF}}$ [%] ^a
400 °C (A)	4.83	0.25×10^{-6}	126 ± 5	no	22
450 °C (B)	4.9	0.9×10^{-6}	208 ± 3	$23, 5 \pm 0, 7$	15
500 °C (C)	5.03	2.0×10^{-6}	96 ± 1	$3, 5 \pm 2$	15.8
550 °C (D)	4.98	15×10^{-6}	no	1361 ± 12	4.8
600 °C (E)	4.94	83×10^{-6}	$13 \pm 0, 5$	1092 ± 18	0.4

^a Sheet conductivity change upon illumination by 15 ns laser pulse at 248 nm.

For comparison, that fastest electric photoresponse of pure ZnO film we obtained in previous study upon the excitation by 15 ns pulse at 355 nm showed the fast and slow components kinetics of $\tau_{fast} = 140 \pm 80 \mu$ s and $\tau_{slow} = 1.3 \pm 0.01$ ms, correspondingly [12].

The most of existing SAW based photodetectors use the concept of a single pass interaction of the acoustic wave with photosensitive layer and the UV light detection efficiency of such sensor does not exceed the one of the corresponding resistive type photodetector built in to acoustic channel. Moreover, the highly photosensitive ZnO layers normally however show inadmissibly slow photoresponse and long recovery times of 2.4–30 s and only in rare studies faster responses were achieved [7–11]. By exploiting the approach of multiple SAW reflections one may obtain detectors with simultaneously fast photoresponse and high sensitivity to UV light [12].

A dosing of ZnO by Mg atoms results in enlargement of the band gap up to ~ 4.05 eV at 49 mol% of Mg [13] and therefore photoresponse may be shifted to ~ 220 – 260 nm range [14]. However the Mg doping results in gradual decrease of conductance which diminishes the acoustoelectric interaction in SAW sensors. Moreover, at Mg atoms content higher than ~ 30 at mol% numerous defects in crystalline structure of ZnO are formed, which causes a degradation of optical properties [15]. The simultaneous doping of ZnO by Mg and Al atoms may assist in tuning electrical, optical and structural properties of ZnO in wide range. $Zn_{1-x-y}Mg_xAl_yO$ deep UV sensitive films are expected to contribute substantially to enhancement of SAW UV photodetector performance. In particular, the band gap is changed by the increase of the Mg content similar to ZnMgO and the conductivity can be controlled by the variation of the x/y ratio in $Zn_{1-x-y}Mg_xAl_yO$ oxide. In particular, $Zn_{0.96-x}Mg_xAl_{0.04}O$ ($x = 0.25$) films show both a band gap as wide as 4.5 eV and the resistance as low as $6 \times 10^{-3} \Omega \times cm$ [16]. The alteration of Al concentration does not result in significant change of the band gap. For Zn(Mg, Al)O films with 10 mol% Mg atoms the crystalline structure quality remains high when the Al content does not exceed ~ 4 – 5 at mol% [16].

The UV ‘on/off’ conductivity of Zn(Mg, Al)O film should be not too low and not high to be obtain effective SAW photodetector. Indeed, in case of low electron concentration, i.e. at high Mg content the wave passes through the material almost without attenuation. And vice-versa a SAW is too much attenuated when the film is too much doped by Al and initial conductivity is high. The compromise can be found when multiple SAW reflections are used for UV detection [12]. Alternatively, as we shown in further

discussion, by moderate Al doping at ~ 1 at% and by changing the film growth temperature one may tune the initial sheet conductivity of Zn(Mg, Al)O film in broad range passing through the maximum of SAW attenuation and also two more important ranges where attenuation alters nonlinear under illumination by UV light. As there are many variable parameters which are capable significantly change the properties of this complex oxide we had to fix several of them and carefully study the influence of only one of them, namely, a temperature of growth. We however choose a fixed concentration of Mg atoms guided by the following arguments. We aimed to obtain an oxide with maximal blue shift of the band gap without significant degradation of the oxide crystalline structure and moderate acoustoelectric interaction with SAW. Thus, it is preferable, that Mg atoms content is lower than ~ 30 – 25 at mol% [15]. A bit lower Mg content compared to [16] was chosen to guarantee better quality of crystalline structure and optical properties of films. Apart from dopant induced conductivity change the temperature and oxygen ambient pressure much influence the structural, optical properties and film deficiency which all influence the kinetics of photoelectric response.

We study optical, structural and photoelectric properties of Zn(Mg, Al)O films on LiNbO₃ substrates grown by PLD method at varied temperature. The deposition regime is optimized to produce highly deep UV sensitive films with short photoelectric response/relaxation times, which also meet the strict requirements to be integrated to SAW photodetector.

2. Experimental details

$Zn_{1-x-y}Mg_xAl_yO$ films were prepared YX-128° LiNbO₃ piezoelectric substrates by using pulsed laser deposition (PLD) method. Ceramic $Zn_{0.74}Mg_{0.25}Al_{0.01}O$ was prepared by mixing ZnO, MgO and Al₂O₃ powders from AlfaAesar (99.998%) and annealing at 1150 °C during 5 h followed by 2 h annealing at 1450 °C. KrF laser radiation (248 nm, 15 ns) was focused on the rotating Zn(Mg, Al)O target to get a 2×5 mm spot with fluence of $2 J cm^{-2}$. The 1×2 cm YX-128° LiNbO₃ substrate was positioned at 5 cm from the target and its temperature was controlled between 400 °C and 600 °C (the samples are named A, B, C, D and E as shown in table 1). The chamber was evacuated to the base pressure of

5×10^{-4} mbar and 250 nm thick Zn(Mg, Al)O films were deposited for 4000 laser shots at oxygen ambient pressure of 10^{-1} mbar. Similar ZnMgAlO films were also *in situ* deposited on the double side polished fused silica substrates together with each Zn(Mg, Al)O/LiNbO₃ sample. These Zn(Mg, Al)O/SiO₂ films were used to characterize the films optical transmission in deep UV range where LiNbO₃ is not transparent. Note, that oxygen pressure of 10^{-1} mbar was experimentally found to be most appropriate to obtain the Zn(Mg, Al)O film for a SAW channel. To discover this deposition regime several preliminary tests were done. In particular, the films prepared at 500 °C and at $2\text{--}5 \times 10^{-2}$ mbar of oxygen show $\sim 3\text{--}2$ orders of magnitude higher conductivity compared to those obtained at 10^{-1} mbar. As a consequence for all the films prepared at oxygen pressure lower than 10^{-1} mbar a SAW is heavily attenuated by film and it can't reach the output IDT. The x-ray diffraction (XRD) measurements were done by using D2 PhaserBruker x-ray diffractometer equipped with positionsensitive detector LYNXEYE with Cu K α radiation at 30 kV and 10 mA. The scan step was 0.01°. Optical transmission of Zn(Mg, Al)O/SiO₂ films was characterized by using UV/vis Spectrophotometer Agilent Technologies HP-8453. The SAWs were generated in YX-128° LiNbO₃ piezoelectric substrates by using interdigital transducers (IDTs) with central frequency of 120.7 MHz and a photoacoustic response was measured by using a network analyzer OBZOR 304/1 similar to procedure described elsewhere [12]. The deep UV sensitive Zn(Mg, Al)O films were excited by using radiation of single mode CW HeCd laser Kimmon IK3501R-G (325 nm, 25 mW cm⁻²) and UV light emitting diode (267 nm, 1.4 mW). The photoelectric response kinetics in films was studied upon the excitation by KrF laser pulse (248 nm, $\sim 500 \mu\text{J cm}^{-2}$, 15 ns). The used deep UV radiation penetrates only for less than ~ 100 nm to ZnMgAlO and is entirely absorbed by studied Zn(Mg, Al)O films. The possible absorption induced heating may effect only a SAW phase but not the attenuation. SAW attenuation is the product of only electro-acoustic interaction in studied structures. Therefore we do not account the heating effect here as a minor.

3. Results and discussion

3.1. Structural properties of Zn(Mg, Al)O films

The XRD spectra of Zn(Mg, Al)O/LiNbO₃ films shown in figure 1(a) reveal peaks at 34.7° and 42.55° corresponding to ZnMgO (002) of wurtzite phase peak and ZnMgO (200) of cubic phase. The more intense lines of single crystalline LiNbO₃ substrate in raw XRD spectra shown in the figure 1(a) inset were subtracted for simplicity of presenting.

Upon the substitution of the larger Zn²⁺ (0.60 Å) ions by the smaller Mg²⁺ (0.57 Å) ones in wurtzite structure the typical (002) reflex of ZnO at 34.5° which is also observed for pure ZnO/LiNbO₃ reference sample is shifted to be 34.7° and is assigned as (002) peak of ZnMgO.

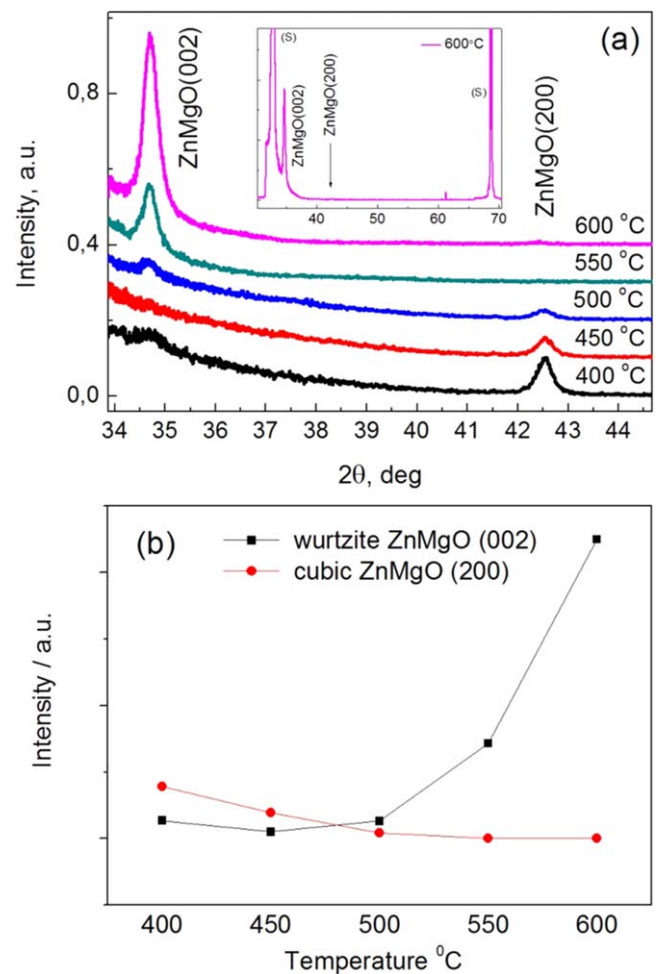


Figure 1. (a) XRD pattern of ZnMgAlO films (a) and intensity of (002) ZnMgO wurtzite phase and (200) ZnMgO cubic phase. XRD spectrum of Sample E is shown in inset. Substrate peaks are marked as (S). (b) (002) ZnMgO wurtzite and (200) ZnMgO cubic phase XRD peaks normalized to intensity of (104) LiNbO₃ reflex as a function of film synthesis temperature.

Films grown at higher temperature of 600 °C reveal only intense (002) ZnMgO reflex whereas (200) reflex of ZnMgO cubic phase is not observed as shown in figure 1. Thus, at these growth conditions Mg²⁺ ions readily substitute Zn²⁺ ones in wurtzite lattice of ZnO and the ZnMgO cubic phase is not produced. For films grown at reduced temperature the intensity of (002) ZnMgO reflex is gradually decreased and (002) peak is hardly noticed already at 400 °C, which claims that the wurtzite structure degradation occurs. The (200) ZnMgO cubic phase reflex is in opposite increased at lower temperature which evidences the film structure changes from wurtzite to cubic ZnMgO. However the XRD intensity of ZnO related peaks is decreased evidencing the overall degradation of the films crystallinity at reduced growth temperature.

3.2. Optical properties and photoelectric response of Zn(Mg, Al)O thin films

As shown in figure 2 the optical transmission spectra of Zn(Mg, Al)O films reveal overall absorption edge at

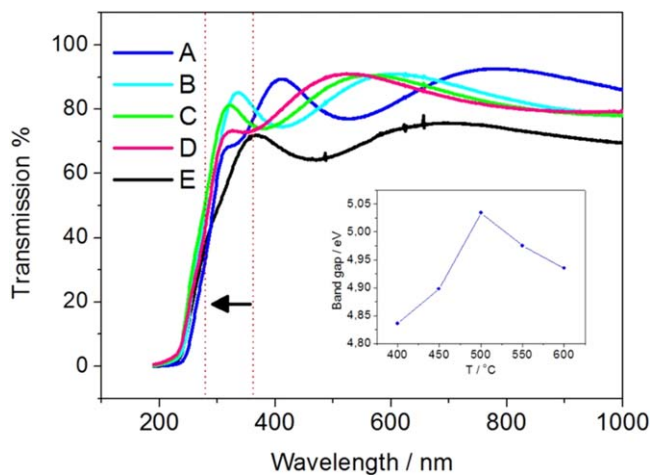


Figure 2. Optical transmission spectra of Zn(Mg, Al)O films grown at different temperatures. The band gap energies extracted from transmission data for corresponding films are shown in the inset. The blue shift of the transmission spectra compared to pure ZnO is shown by arrow.

$\sim 265\text{--}270$ nm which is ~ 100 nm deeper in UV compared to 365 nm typical for pure ZnO. The band gap energies (E_g) were determined from the fits of the corresponding plots of $(\alpha h\nu)^2$ versus $h\nu$ (see figure S1 in supplementary material for more detail is available online at stacks.iop.org/SMS/28/065024/mmedia) using the procedure described elsewhere [17]. The extracted band gap values are summarized in table 1. The dependence of the band gap as a function of the films growth temperature is shown in the figure 2 inset. In particular the largest band gap for studied series is 5.03 eV for films grown at 500 °C, which is more than 1.5 eV larger compared with 3.37 eV for pure ZnO.

The most significant effect of Mg atoms dosing on the band gap energy increase is in a good agreement with previous study of Zn(Mg, Al)O films [15]. The minor alterations of the band gap energy of $\sim 0.05\text{--}0.1$ eV shown in the figure 2 inset are likely related to more complicated structural changes due to growth temperature variation. Indeed, the films grown at 600 °C reveal only intense (002) ZnMgO reflex, indicating that the wurtzite phase is predominant. Lowering the growth temperature to 400 C results in (i) the decrease of ZnMgO wurtzite phase and an increase of ZnMgO cubic phase content as well as (ii) the overall degradation of crystalline structure. We speculate that these above phase transformations and the alteration of crystalline phases ratio in film are responsible for detected minor fluctuations in the band gap energy.

Having poor crystalline structure the ZnMgAlO films grown at low temperatures however show much better photoelectrical characteristics compared to their wurtzite counterparts prepared at 600 °C. The amount of defect states which function as traps for carriers recombining upon UV excitation is lowered at reduced growth temperature. As a result the films sintered at 400 °C–500 °C and excited by 248 nm laser pulses show very fast photo-response of $\sim 0.1\text{--}0.2$ ms and a minor/absent millisecond component as shown in figure 3 and table 1. Moreover, those films show higher sensitivity toward 248 nm radiation. For comparison, the relative sheet

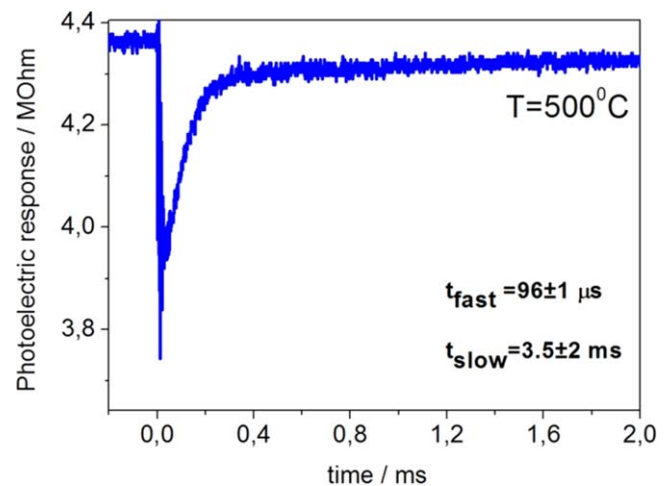


Figure 3. Typical photoelectric response of Zn(Mg, Al)O film grown at 500 °C (sample C) upon the excitation by 15 ns laser pulse at 248 nm.

conductivity change $\Delta\sigma/\sigma_{\text{dark}}$ for samples grown at 400 °C–500 °C was $\sim 22\%$, which is much larger than $\sim 0.4\%$ measured for films prepared at 600 °C.

The sample C with largest bandgap in series corresponds to film with intermediate ratio of wurtzite, cubic and amorphous phases of $\text{Zn}_{1-x-y}\text{Mg}_x\text{Al}_y\text{O}$. Interesting, that films prepared in this regime show the fastest photoresponse.

On the other hand, samples grown at higher temperatures show slower photoelectric response. The longer carriers relaxation evidence the presence of long-living states in the band gap, which significantly increase the recovery time of the photodetector.

3.3. Electrical and photoacoustic characteristics of Zn(Mg, Al)O/LiNbO₃ structures

UV light induced SAW attenuation change $\Gamma(\sigma_{\text{UV}}) - \Gamma(\sigma_{\text{dark}})$ in ZnMgAlO/LiNbO₃ delay line as a function of illumination intensity measured at frequency of 120 MHz at 267 and 325 nm were extracted from corresponding S_{21} characteristics as shown in figure 4. The corresponding raw data of S_{21} characteristics is shown in the figure S4 of supplementary material.

Remarkably that for Zn(Mg, Al)O films obtained at 500 °C and 550 °C SAW attenuation is decreased at higher UV light illumination intensity at both wavelength as shown in figures 4(a) and (b). For films grown at 400 °C and 450 °C the SAW attenuation is in opposite increased under UV light illumination, which corresponds to the typical behavior of photosensitive ZnO layer [12]. Summarizing both results one can conclude that the SAW attenuation in photodetector with film obtained at 550 °C and 400 °C which have the initial sheet conductivity of $15 \times 10^{-6} (\Omega/\square)^{-1}$ and $0.25 \times 10^{-6} (\Omega/\square)^{-1}$ are greater changed with increase of the UV illumination intensity and the change of $\Gamma(\sigma_{\text{UV}}) - \Gamma(\sigma_{\text{dark}})$ shows the opposite signs at that (see figures 4(a) and (b)).

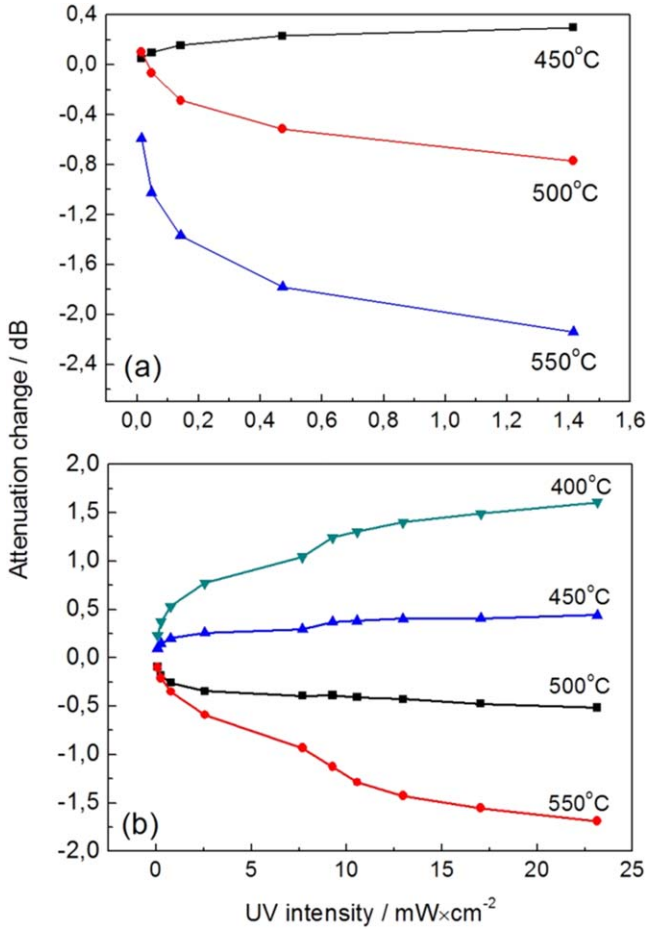


Figure 4. (a) UV light induced SAW attenuation change $\Gamma(\sigma_{UV}) - \Gamma(\sigma_{dark})$ as a function of light intensity measured at frequency of 120 MHz for (a) samples B, C and D under illumination by 267 nm diode and (b) samples A, B, C and D under illumination by 325 nm (HeCd laser).

Extra carriers are generated in the Zn(Mg, Al)O layer under illumination by UV light. SAW velocity change (Δv) and wave intensity attenuation (Γ) induced by acoustoelectric interaction are given by [17, 18]

$$\frac{\Delta v}{v_0} = \frac{k_{ef}^2}{2} \frac{1}{1 + \sigma_{sh}^2 / \sigma_M^2}, \quad (1)$$

$$\Gamma = k_{ef}^2 \left(\frac{2\pi}{\lambda} \right) \frac{\sigma_{sh} / \sigma_M}{1 + \sigma_{sh}^2 / \sigma_M^2}, \quad (2)$$

where v_0 , λ , σ_{sh} , $k_{ef}^2 = 0.056$ and $\sigma_M = v_0(\epsilon_s + \epsilon_0) = 1.48 \times 10^{-6} (\Omega/\square)^{-1}$ denote a SAW initial velocity in LiNbO₃ (3880 m s⁻¹), wavelength, sheet conductivity of Zn(Mg, Al)O layer, effective electromechanical coupling coefficient and the material constant, respectively. Dielectric permittivity of LiNbO₃ substrate $\epsilon_s = 3.7 \times 10^{-10}$ F m⁻¹. When the sheet conductivity of the photosensitive Zn(Mg, Al) O film limits to σ_M value the attenuation Γ of a SAW reaches a maximum. The initial sheet conductivities of the films prepared at different temperatures and the data of theoretical modeling according to formula (2) are shown in figure 5.

In case of pure n-type ZnO the absorption of UV photon results in generation of extra electrons in conduction band

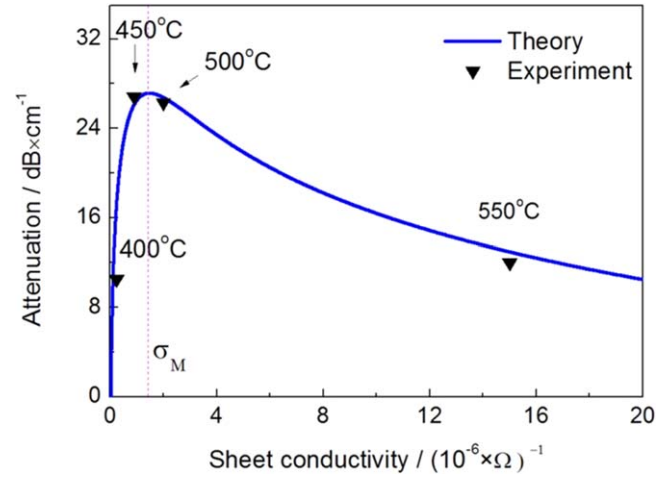


Figure 5. SAW attenuation (per propagation length unity) as a function of initial sheet conductivity of a film. Measured values for initial sheet conductivity of Zn(Mg, Al)O films prepared at 400 °C (A), 450 °C (B), 500 °C (C) and 550 °C (D) are marked by dots and its variation induced by 248 nm laser pulse 500 μJ cm⁻² is shown by section. The theoretical model according to formula is shown by solid curve (2).

which mostly define the photocurrent. The presence of more native +2 charged oxygen vacancies in film results in larger electronic concentration and increased conductivity [19]. Long living defect states are charged upon the absorption of UV photons which additionally influence the carriers relaxation kinetics. In particular, the charged vacancies influence on the ZnO electronic conductivity similar to positive bias applied to field effect transistor with ZnO channel and isolated photo-gate, i.e. do further increase the conductivity. The relaxation kinetics becomes also slower due to existence of the charged long living defect states. Therefore, normally pure ZnO films with high oxygen deficiency show slower photoresponse compared to defect free counterpart.

As we showed earlier the initial sheet conductivity of pure ZnO films, i.e. without UV light, is smaller than σ_M value and it is always increased with UV light intensity. The pure ZnO films with larger amount of long living trap states show greater initial (dark) SAW attenuation because of higher film conductivity and more significant conductivity change upon UV light illumination [12]. The conductivity does likely approach but not pass the maximum of attenuation Γ . Therefore a SAW is always greater attenuated with conductivity increase [12, 20]. It happens because the variation of sheet conductivity of pure ZnO can be only slightly varied by control of oxygen vacancies amount, which is not enough to reach the maximum of the $\Gamma(\sigma_{sh})$ characteristics.

The sheet conductivity of ZnMgAlO films discussed here may in contrast be tuned in quite broad range of $0.25 \times 10^{-6} (\Omega/\square)^{-1}$ to $83 \times 10^{-6} (\Omega/\square)^{-1}$ by variation of the film growth temperature from 400 °C to 600 °C. Interesting that the value $\sigma_M = 1.48 \times 10^{-6} (\Omega/\square)^{-1}$ which corresponds to SAW attenuation maximum for studied delay line is within the range of the studied Zn(Mg, Al)O films conductivity variation. In particular Samples A and B have smaller and Samples C, D and E have larger initial conductivity than σ_M .

Indeed, for the Samples A and D grown at 400 °C и 550 °C have initial sheet conductivity of $0.25 \times 10^{-6} (\Omega/\square)^{-1}$ and $15 \times 10^{-6} (\Omega/\square)^{-1}$, which corresponds to the abrupt positive and more gentle negative slopes of $\Gamma(\sigma)$ characteristics. Upon the illumination by UV light the SAW is better attenuated because of larger variation of $\Gamma(\sigma_{sh})$. The positive and negative slopes also explain the different signs of SAW attenuation change observed for samples A, B compared to C, D. For Samples B and C grown at 450 °C and 500 °C with initial sheet conductivity of $0.9 \times 10^{-6} (\Omega/\square)^{-1}$ and $2 \times 10^{-6} (\Omega/\square)^{-1}$ SAW attenuation is in opposite does not much under UV light illumination because these samples correspond to flat top of the $\Gamma(\sigma_{sh})$ characteristics. Thereby varying a growth temperature of Zn(Mg, Al)O films one may alter the film sheet conductivity in quite wide range and therefore tune the 'working point' close to abrupt slope of $\Gamma(\sigma_{sh})$ to obtain best sensitivity of UV SAW detector. Note, that pure ZnO films designed at our previous studies [12] prepared at varied temperatures always showed higher attenuation at increased UV illumination intensity and $\Gamma(\sigma_{UV}) - \Gamma(\sigma_{dark})$ never changed the sign for all the films grown at various temperatures.

A comparison with Ga₂O₃ which is being a natural solar-blind material with a bandgap of 4.9 eV is another promising candidate for deep UV sensitive photodetecting, seems to be relevant here. In particular, the early photodetectors with Ga₂O₃ layer sensitive to 254 nm showed the slow photo-current decay kinetics with characteristic time constants of ~1 and 16 s for fast and slow components, correspondingly, related to long living traps in the band gap [21]. The later improvement of Ga₂O₃ based devices resulted in excellent light sensitivity of ~3 A/W and faster photoresponse of 18 ms [22]. For comparison the fastest photoelectric response for the Zn_{1-x-y}Mg_xAl_yO films presented in this paper is at least ~6 fold faster with characteristic time constants of ~0.1 and ~3.5 ms for corresponding fast and slow components. Normally pure oxides such as ZnO, which have a lot of long lining defect states do show a higher UV light sensitivity [12]. Therefore in many semiconductor based photodetectors there is a tradeoff between fast and sensitive photodetector. As we showed recently SAW based detectors provide an alternative approach to solve this problem when the multiple SAW reflections are exploited [12]. Thus, in some applications Zn_{1-x-y}Mg_xAl_yO films with bandgap of ~5 eV and sub-millisecond photoresponse may concur with Ga₂O₃ films. The use of Ga₂O₃ as a photosensitive layer in SAW based detectors is another prospective subject for studies, which likely could result in further optimization of the deep UV photodetectors performance. Indeed, the preparation process of Zn_{1-x-y}Mg_xAl_yO films needs precise control of more experimental parameters compared with Ga₂O₃. However, many parameters such as Mg and Al concentrations, growth temperature and amount of oxygen defects provide broad-possibilities to tune the properties of the complex Zn_{1-x-y}Mg_xAl_yO oxide to meet requirements of particular application. The study of these many deposition regimes still needs a systematic characterization and is beyond the focus of the present paper. Here we only show that even for given Mg

and Al concentrations and oxygen pressure the photo-electric properties can be successfully tuned in a broad range by varying the growth temperature and the abrupt slopes of $\Gamma(\sigma_{sh})$ characteristics play a key important role in the performance of a SAW based photodetector.

4. Conclusions

In summary, the optical absorption band edge of Zn_{1-x-y}Mg_xAl_yO films was shifted to ~5 eV (265 nm) by Mg doping. The temperature range to obtain detector with fast photoelectric response of 0.1–0.2 ms towards 248 nm laser light was found. The sensitivity and photoresponse time of UV SAW detector is optimized by changing the growth temperature and thereby tuning the sheet conductivity of Zn(Mg, Al)O film in a broad range of $0.25 \times 10^{-6} (\Omega/\square)^{-1}$ to $83 \times 10^{-6} (\Omega/\square)^{-1}$ passing by two abrupt slopes of $\Gamma(\sigma_{sh})$ characteristics where SAW attenuation alteration is maximal. The studied Zn(Mg, Al)O films are promising sensitive elements of deep UV SAW photodetectors and photoelectric detectors of other types.

Acknowledgments

This research work is supported by Ministry of Science and Higher Education of the Russian Federation project No. 16.5405.2017/8.9. V E Kaydashev acknowledge postdoctoral program in frame of Government of Russian Federation (Agreement № 074-02-2018-286) for partial support of his research.

ORCID iDs

V E Kaydashev  <https://orcid.org/0000-0003-1913-591X>

K G Abdulvakhidov  <https://orcid.org/0000-0001-6697-9192>

V A Irkha  <https://orcid.org/0000-0002-6474-8240>

References

- [1] Fu C, Lee J, Lee K and Yang S 2015 Low-intensity ultraviolet detection using a surface acoustic-wave sensor with a Ag-doped ZnO nanoparticle film *Smart Mater. Struct.* **24** 015010
- [2] Huang T and Ma C 2008 Characterization of response of ZnO/LiNbO₃-based surface acoustic wave delay line photodetector *Japan. J. Appl. Phys.* **47** 6507
- [3] Sharma P and Sreenivas K 2003 Highly sensitive ultraviolet detector based on ZnO/LiNbO₃ hybrid surface acoustic wave filter *Appl. Phys. Lett.* **83** 3617
- [4] Tsai W C, Kao H L, Liao K H, Liu Y H, Lin T P and Jeng E S 2015 Room temperature fabrication of ZnO/ST-cut quartz SAW UV photodetector with small temperature coefficient *Opt. Express* **23** 2187

- [5] Kumar S, Kim G H, Sreenivas K and Tandon R P 2009 ZnO based surface acoustic wave ultraviolet photo sensor *J. Electroceram.* **22** 198
- [6] Emanetoglu N W, Zhu J, Chen Y, Zhong J, Chen Y and Lu Y 2004 Surface acoustic wave ultraviolet photodetectors using epitaxial ZnO multilayers grown on r-plane sapphire *Appl. Phys. Lett.* **85** 3702
- [7] Peng W, He Y, Wen C and Ma K 2012 Surface acoustic wave ultraviolet detector based on zinc oxide nanowire sensing layer *Sensors Actuators A* **184** 34
- [8] Chivukula V, Ciplys D, Shur M and Dutta P 2010 ZnO nanoparticle surface acoustic wave UV sensor *Appl. Phys. Lett.* **96** 233512
- [9] Peng W, He Y, Xu Y, Jin S, Ma K, Zhao X, Kang X and Wen C 2013 Performance improvement of ZnO nanowire based surface acoustic wave ultraviolet detector via poly (3,4-ethylenedioxythiophene) surface coating *Sensors Actuators A* **199** 149
- [10] He X L, Zhou J, Wang W B, Xuan W P, Yang X, Jin H and Luo J K 2014 High performance dual-wave mode flexible surface acoustic wave resonators for UV light sensing *J. Micromech. Microeng.* **24** 055014
- [11] Pang H F, Fu Y Q, Li Z J, Li Y F, Ma J Y, Placido F, Walton A J and Zu X T 2013 Love mode surface acoustic wave ultraviolet sensor using ZnO films deposited on 36° Y-cut LiTaO₃ *Sensors Actuators A* **193** 87
- [12] Karapetyan G Y, Kaydashev V E, Zhilin D A, Minasyan T A, Abdolvakhidov K G and Kaidashev E M 2017 Use of multiple acoustic reflections to enhance SAW UV photo-detector sensitivity *Smart Mater. Struct.* **26** 035029
- [13] Park W I, Yi G C and Jang H M 2001 Metalorganic vapor-phase epitaxial growth and photoluminescent properties of Zn_{1-x}Mg_xO (0 < x < 0.49) thin films *Appl. Phys. Lett.* **79** 2022
- [14] Endo H, Kikuchi M, Ashioi M, Kashiwaba Y, Hane K and Kashiwaba Y 2008 High-sensitivity mid-ultraviolet Pt/Mg_{0.59}Zn_{0.41}O Schottky photodiode on a ZnO single crystal substrate *Appl. Phys. Express* **1** 051201
- [15] Kim I S and Lee B T 2010 Design and growth of deep UV-range single crystalline ZnMgAlO thin films lattice-matched to ZnO *Cryst. Growth Des.* **10** 3273
- [16] Yang C, Li X M, Gao X D, Cao X, Yang R and Li Y Z 2011 ZnMgAlO based transparent conducting oxides with modulatable bandgap *Solid State Commun.* **151** 264–7
- [17] Wixforth A, Scriba J, Wassermeier M, Kotthaus J P, Weimann G and Schlapp W 1989 Surface acoustic waves on GaAs/Al_xGa_{1-x}As heterostructures *Phys. Rev. B* **40** 787
- [18] Wixforth A, Kotthaus J P and Weimann G 1986 Quantum oscillations in the surface acoustic-wave attenuation caused by a two-dimensional electron system *Phys. Rev. Lett.* **56** 2104
- [19] Liu L, Mei Z, Tang A, Azarov A, Kuznetsov A, Xue Q K and Du X 2016 Oxygen vacancies: the origin of n-type conductivity in ZnO *Phys. Rev.* **93** 235305
- [20] Huang T Y and Ma C C 2008 Characterization of response of ZnO/LiNbO₃-based surface acoustic delay line photodetector *Japan. J. Appl. Phys.* **47** 6507
- [21] Guo D et al 2014 Fabrication of β-Ga₂O₃ thin films and solar-blind photodetectors by laser MBE technology *Opt. Mater. Express* **4** 1067
- [22] Guo D et al 2018 Self-powered ultraviolet photodetector with superhigh photoresponsivity (3.05 A/W) based on the GaN/Sn:Ga₂O₃ pn junction *ACS Nano* **12** 12827